

# Nanostructured $p$ - $n$ Junctions for Printable Photovoltaics

Christoph J. Brabec, Thomas Nann, and Sean E. Shaheen

## Abstract

By controlling the morphology of organic and inorganic semiconductors on a molecular scale, nanoscale  $p$ - $n$  junctions can be generated in a bulk composite. Such a composite is typically called a bulk heterojunction composite, which can be considered as one virtual semiconductor combining the electrical and optical properties of the individual components. Solar cells are one attractive application for bulk heterojunction composites. Conjugated polymers or oligomers are the favorite  $p$ -type semiconducting class for these composites, while for the  $n$ -type semiconductor, inorganic nanoparticles as well as organic molecules have been investigated. Due to the solubility of the individual components, printing techniques are used to fabricate them.

**Keywords:** conjugated polymers, hybrid photovoltaics, mesoporous oxides, nanoparticles, nanostructure, organic photovoltaics, photoinduced charge transfer.

## Introduction

The increasing global consumption of energy and decreasing fossil fuel resources are driving research in the area of regenerative energy sources. Among the alternatives, solar energy conversion takes a prominent role because it is globally available and inexhaustible, and the electrical energy can be easily converted to other energy-transfer media (e.g., hydrogen). It would be indeed intriguing and highly attractive to imagine photovoltaic elements based on thin plastic carriers, manufactured by printing and coating techniques and packaged using lamination techniques. Solution-processable organic and inorganic semiconductors have a high potential to fulfill these requirements.

Most organic semiconductors are intrinsic semiconductors, and the primary excitation is a Coulomb bound exciton. Photovoltaic cells made from single organic semiconductors therefore achieve tiny power-conversion efficiencies and low incident-photon-to-current or external

quantum efficiencies (EQEs). A solution was only found in 1995, when several groups independently showed that the EQE could be enhanced by several orders of magnitude by blending two materials with relative preferences for positive and negative charges.<sup>1</sup> The difference in electron affinities creates a driving force at the interface between the two materials that is strong enough to split photogenerated excitons. By blending materials on a nanostructured scale ( $\sim 10$  nm), the interface is distributed throughout the device. The separated charges must then travel through the appropriate material toward the contacts. The concept of blending  $p$ -type semiconductors with  $n$ -type semiconductors has become popular under the name "bulk heterojunction composites."

The EQE represents that fraction of photoexcitations that survive both charge separation and transport processes. Using the bulk heterojunction concept, the EQE has been increased from 29%<sup>1</sup> to 50%,<sup>2</sup> and

recently an EQE of 80% was reported.<sup>3</sup> These impressively high values have been obtained for blends of conjugated polymers with fullerenes.

Solution processing may qualify polymeric photovoltaics as an alternative renewable energy source. Unfortunately, overall power-conversion efficiencies under normalized solar conditions are low. The highest efficiencies obtained today are only about 3.5%,<sup>4</sup> clearly below the critical 5% benchmark. The main reason for this disappointingly low power efficiency despite the high EQE is the spectral mismatch of the organic absorbers to the solar spectrum.

Effective light harvesting in a blended photovoltaic device demands efficient charge separation and transport. First, the energy bands of the two materials have to cascade in order to guarantee charge generation after photoexcitation. Second, each material must provide a continuous path for the transport of separated charge to the contacts. This demands a highly complex morphology between the two compounds with interconnected domains in the nanometer scale to prevent trapping and more ordered regions in the 100 nm scale to guarantee efficient transport channels.

In the following, we will discuss three different approaches to the realization of solution-processable bulk heterojunction solar cells: one fully organic approach and two hybrid approaches utilizing inorganic  $n$ -type nanoparticles and  $p$ -type semiconducting polymers.

## Organic Bulk Heterojunctions

Fullerenes have interesting properties with respect to organic photovoltaic devices. They can be processed from solution, they are available at high purity, they are one of the rare environmentally stable  $n$ -type semiconductors, and finally, they show a sufficiently high electron mobility. Among the more intensively investigated fullerenes are the methanofullerenes, mainly because of their excellent solubility. In blends with prototype semiconducting polymers, photoinduced charge transfer is observed within 20 fs, while recombination is significantly slower, typically in the nanosecond to microsecond regime.

One of the main concerns for bulk heterojunction composites is the morphology of the photoactive layer, namely, the formation of a nanostructured three-dimensional interpenetrating network between the two components. Phase separation and the possible formation of fullerene nanocrystallites are expected to occur upon film formation by spin-coating or printing techniques. A proper tool to investigate the morphology of such films in

the nanoscale is atomic force microscopy (AFM).

Simply changing the spin-coating solvent from xylenes to chlorobenzene and dichlorobenzene significantly changes the morphology, as shown by the AFM pictures in Figure 1 in the case of 100-nm-thick films that consisted of MDMO-PPV [poly-(2-methoxy-5-(3',7'-dimethyloctyloxy))-1,4-phenylene vinylene] and phenyl-C61-butyric acid methyl ester (PCBM).

In general, better fullerene solvents yield smoother films. Xylenes (Figure 1c) and toluene (not shown) already give rise to large defects in the form of deep pinholes (>5 nm, not visible in Figure 1c) and phase separation in the 100 nm range or more. For an intermediate solvent (chlorobenzene, CB, Figure 1b), surface structures indicate phase separation and domain formation in the 100 nm range or smaller, while the best solvent (ortho-dichlorobenzene, ODCB, Figure 1a) gives rise to an intimately mixed morphology in the 10 nm scale.

The characterization of photovoltaic devices (Table I) with an active layer as depicted in Figure 1 allows a discussion of the correlation between morphology and performance in bulk heterojunction devices. The better photovoltaic devices with efficiencies ( $\eta$ ) exceeding 3% are obtained from the "better" solvents (i.e., CB and ODCB), due to an increased short-circuit current ( $I_{sc}$ ) and a better fill factor. Both  $I_{sc}$  and the fill factor are strongly influenced by the morphology of the photoactive blend. An optimal morphology consists of an interpenetrating network with a scale of phase separation that matches the exciton diffusion length and that also yields pathways for the rapid

transport of carriers out of the photoactive layer. The exciton diffusion length for conjugated polymers is typically in the 10 nm range or smaller. Assuming a typical carrier lifetime ( $\tau$ ) of 1  $\mu$ s and an average carrier mobility ( $\mu$ ) of  $10^{-5}$  cm<sup>2</sup>/V s (as measured for MDMO-PPV), the carrier drift length ( $d$ ) at a built-in field ( $E$ ) of  $\sim 10^5$  V/cm (short-circuit conditions) is  $d = \mu\tau E > 10$  nm. Note that the exciton diffusion length and the carrier drift length are in concurrence with each other with respect to forming an optimum morphology. For efficient charge generation, a phase separation of the donor and acceptor below the exciton diffusion length is favorable to guarantee complete charge separation. For the efficient transport of single carriers, larger domains of pristine components will reduce scattering and recombination and enhance transport properties. Thus, there is only a small dimensional window for the optimum morphology. For the specific semiconductors discussed here, the better solvents seem to better fulfill these conditions with respect to morphology. Interestingly, the highest short-circuit currents are observed for a morphology with domain sizes between 10 nm and 100 nm (CB). Too-intimate mixing of the two components (ODCB) might generate transport losses like frequent scattering or trap-assisted recombination.

Controlling the morphology in the nanometer regime is a key parameter for efficient organic photovoltaic devices. Two contradictory mechanisms have to be compatibilized into one thin-film layer. Domains that are too large can hamper the formation of charge carriers (the exciton diffusion lengths in *p*-type and *n*-type semiconductors), while domains that are too small can induce transport losses.

## Hybrid Bulk Heterojunctions with "Soluble" Nanoparticles

Semiconductor nanocrystals with diameters in the lower nanometer size range display three types of properties: first, properties that can be attributed to their small size (referred as "molecular properties" in the following); second, solid-state properties; and third, mesoscopic phenomena, only observed in nanoscale materials. "Mesoscopic" here means properties that arise from the transition from molecules to bulk crystals. These physical and chemical properties scale with the size of the particles (also called the quantum size effect).

These particular characteristics of semiconductor nanocrystals result in some advantages, enabling many new applications. Due to their size, nanocrystals resemble colloids and molecular and ionic solutions; that is, they are transparent, and the particles form a sediment only very slowly (within the period of months). This represents an advantage for the processing of such colloids, because they can, up to a certain degree, be treated like ordinary chemical solutions. A further advantage is that semiconductor nanocrystals can be prepared cheaply and in large quantities. Complex and expensive process steps such as clean rooms or high-vacuum techniques are not needed. Beyond photovoltaic applications, semiconductor nanocrystals can be applied in catalysis, phosphors, and light-emitting diodes.

**Nanoparticle Chemistry.** In the early 1990s, the first synthesis methods for II-VI semiconductor nanocrystals from organometallic precursors were published.<sup>5</sup> A new feature was the ability to tune the optical properties by varying the size and shape of the nanocrystals. Further-

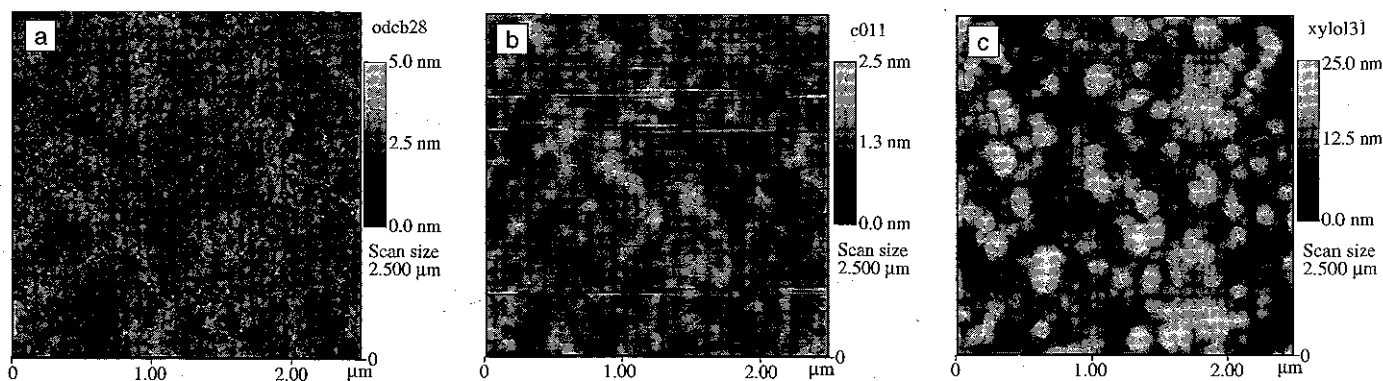


Figure 1. Nanomorphology of organic bulk heterojunction composites: atomic force microscopy (AFM) images of the surface of MDMO-PPV:PCBM (1:4 wt. ratio) composites, spin-cast from 0.4 polymer wt. % solutions. MDMO-PPV is [poly-(2-methoxy-5-(3',7'-dimethyloctyloxy))-1,4-phenylene vinylene]; PCBM is phenyl-C61-butyric acid methyl ester. Solvents used were (a) ortho-dichlorobenzene (ODCB), (b) chlorobenzene (CB), (c) xylenes. The gray scale bars to the right of the images indicate the height of the features shown.

**Table I: Photovoltaic Parameters of MDMO-PPV:PCBM (1:4) Devices.**

	Open Circuit Voltage, $V_{oc}$ (mV)	Short-Circuit Current, $I_{sc}$ (mA/cm <sup>2</sup> )	Fill Factor	Power Efficiency, $\eta$ (%)
Ortho-dichlorobenzene	796	4.46	0.5171	2.294
Chlorobenzene	802	5.37	0.5628	3.034
Xylenes	816	4.16	0.4922	2.09

Notes: MDMO-PPV is [poly-(2-methoxy-5-(3,7-dimethyloctyloxy))-1,4-phenylene vinylene]. PCBM is phenyl-C61-butyric acid methyl ester. Illumination = 80 mW/cm<sup>2</sup> white light (AM1.5 solar simulator, 55°C). Efficiencies are uncorrected for the mismatch between the spectrum of the solar simulator and the true AM1.5 spectrum.

more, the surfaces could be easily modified, paving the way for many novel electro-optical and biomedical applications. Preparations for chalcogenides of the transition metals and III-V semiconductors such as GaAs and InP were published, and first papers reported the successful preparation of ternary systems.

Nanocrystals tend to expel impurities. Due to this self-cleaning effect, no ultra-clean conditions are required for their preparation. The chemical (molecular) properties of colloidal nanocrystals are primarily determined by their surfaces. Therefore, nanocrystals can be dissolved in nearly every solvent by appropriate surface modification. With respect to photovoltaic devices, the particle surface induces the *p-n* junction and therefore should not be passivated for charge transfers. While solution processing is a clear advantage over solid-state solar cells, the depletion effect, or formation of a charge-carrier-depleted zone at the semiconductor interface, in mixed nanocrystal/polymer solutions can be a problem. In some cases, the addition of surfactants or modification of the polymers could become necessary.

**Nanoparticle Physics.** Charge transport within the components and charge transfer between polymers, electrodes, and nanocrystals are crucial for the functionality and efficiency of hybrid photovoltaic devices. The charge-transport properties are primarily characterized by the carrier mobilities and doping of the semiconducting materials; the charge transfer between the components is primarily characterized by the bandgap, the band-edge positions, and the properties of the *p-n* junction.

Generally, the rather low intrinsic mobility of organic semiconductors is regarded as a disadvantage with respect to photovoltaic applications. In inorganic semiconductors, much higher mobility can be observed. Therefore, solution-processable nanoparticles are a sound al-

ternative for photovoltaic applications. Recently, CdSe nanocrystals<sup>6</sup> were used in blends with *p*-type conjugated polymers [e.g., poly(3-hexylthiophene), P3HT] to create novel, nanostructured hybrid bulk heterojunction solar cells.

A further important parameter is the bandgap of the material. Photons with energy higher than the bandgap are broadly absorbed by inorganic semiconductors (also nanocrystals), in contrast to organic molecules, which usually display a relatively narrow absorption feature. Furthermore, the absorption characteristic of the cell can be optimized by choosing a semiconductor with the appropriate bandgap. The bulk bandgaps of the mentioned materials are  $E_g = 1.75$  eV (CdSe, 293 K), 1.53 eV (CuInS<sub>2</sub>, 300 K), 1.49 eV (CdTe, 300 K) and 1.34 eV (InP, 300 K). From this point of view, all of these semiconductors are well suited to photovoltaic applications.

The bandgap of semiconductor nanocrystals scales with the size of the particles. This is observed when the crystal size falls below the size of the Wannier-Mott exciton within the material. In this case, the Bohr radius of the exciton is confined by the size of the nanocrystal. This effect results in an increasing effective bandgap with decreasing particle size. Figure 2a displays this effect, using CdSe nanocrystals of different sizes. Along with the increasing effective bandgap, the absorption edge is blue-shifted with decreasing particle size (from left to right in the figure). In order to enable a spontaneous charge transfer between the hole-conducting polymer and the nanocrystals, the ionization potential  $I_p$  and electron affinity  $E_a$  have to be taken into account. With respect to the electrochemical potential scale,  $I_p$  and  $E_a$  increase with decreasing nanocrystal size (Figure 2b); here, the nanocrystal size decreases from right to left: (a) 3.23 nm, (b) 3.48 nm, (c) 3.73 nm, and (d) 3.80 nm. If these potentials do not meet the photovoltaic requirements, the particle size can be tuned, another semiconductor can be chosen, or

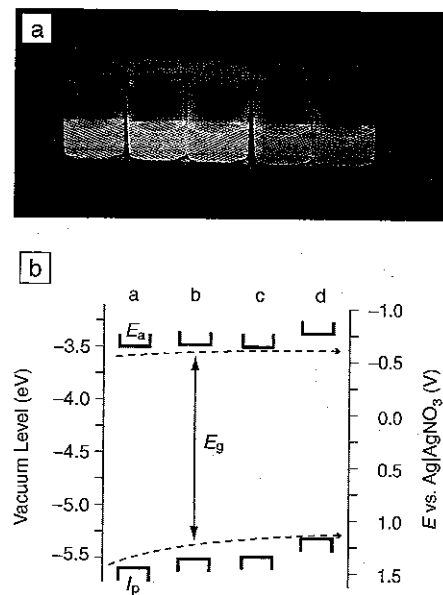


Figure 2. Size effects in colloidal nanocrystals. (a) Photograph of different-sized CdSe nanocrystal colloids in chloroform. The photoluminescence was excited with a UV lamp at 355 nm. (b) Schematic diagram of the electrochemically determined ionization potentials  $I_p$  and electron affinities  $E_a$  of four different sizes of CdSe nanocrystals: a, 3.23 nm; b, 3.48 nm; c, 3.73 nm; d, 3.80 nm.  $Ag/AgNO_3$  is a reference electrode.

the hole-transporting polymer can be changed.

**Nanoparticle Applications to Bulk Heterojunction Solar Cells.** Similar to the fully organic devices, the nanostructured morphology of the nanoparticle-polymer blend is critical in determining device performance. Not surprisingly, the highest performance was found for nanoparticles with a rodlike shape, which allow for longer electron drift lengths within the nanoparticle. Alivisatos et al.<sup>6</sup> demonstrated recently that cylindrical CdSe nanorods with lengths of 50 nm or more significantly improved the photovoltaic performance, as compared with small spherical nanoparticles. Subsequent optimization of the nanoparticles with respect to their transport properties as well as careful selection of suitable *p*-type polymers such as P3HT<sup>6</sup> yielded devices with an EQE of nearly 60% and a power conversion efficiency of 1.7%, impressively confirming the validity of the hybrid bulk heterojunction concept.

Compared to the ideal heterojunction system described earlier, none of the solar

cells published so far fulfills all of the criteria necessary for high power-conversion efficiencies. However, on the basis of these first prototype systems, and given the huge optimization potential of further tuning the electro-optic properties of the components, rapid future improvements are likely to come.

## Hybrid Bulk Heterojunctions with Sintered Nanoparticle Networks

Metal oxide semiconductors such as  $\text{TiO}_2$  are well known for the photocatalytic properties of their surfaces. Correspondingly, the interface between a metal oxide and a conjugated polymer is a potential exciton-dissociating and charge-generating heterojunction. This brings about the possibility of fabricating hybrid metal oxide/conjugated polymer solar cells. As with bulk heterojunction solar cells based on blends of conjugated polymers with fullerenes or nanocrystals, an exciton generated in the polymer must be within about 10 nm of an acceptor interface in order for it to be able to diffuse to that interface and be dissociated. A composite structure consisting of a conjugated polymer intercalated into the pores of a mesoporous metal oxide can provide the necessary morphology to dissociate all the excitons generated in the polymer.

Mesoporous metal oxides can be excellent charge-transfer networks, as demonstrated by the liquid electrolyte dye-sensitized solar cell.<sup>7</sup> In this device, a monomolecular layer of dye is chemisorbed onto the surface of mesoporous  $\text{TiO}_2$ . A liquid electrolyte solution of an iodine/triiodine redox couple dissolved in an organic solvent is used to fill the free spaces of the pores and makes contact to a platinum-coated counter electrode. In the operation of the device, the dye molecules absorb light and inject electrons into the  $\text{TiO}_2$ . The oxidized dye molecules are subsequently reduced by a reaction with the redox species in solution. Transport of the charges out of the device occurs by diffusion of electrons through the  $\text{TiO}_2$  and diffusion/ionic conduction of the redox species to the counter electrode. These devices have achieved 10% efficiency under solar illumination; however, the use of a liquid electrolyte makes them difficult to fabricate on a large scale. Solid-state versions have been fabricated by replacing the liquid electrolyte with an optically transparent hole-transporting polymer,<sup>8</sup> polymer electrolyte,<sup>9</sup> copper salt,<sup>10</sup> or molecular hole transporter,<sup>11</sup> with the last achieving efficiencies of more than 3%.

One of the limiting factors in the performance of these solid-state dye-sensitized solar cells is that a sufficient number of

dye monolayers is necessary for a high optical density. Thus, the devices must be made several micrometers thick. However, transport of holes through an organic semiconductor of this thickness is difficult without the presence of strong electric fields. A conjugated polymer/mesoporous metal oxide composite device is therefore an attractive alternative. Since conjugated polymers have high optical absorption coefficients ( $>10^5 \text{ cm}^{-1}$ ), a composite device that is 50% polymer and 50% metal oxide, for instance, can be a few hundred nanometers thick and still absorb nearly all incident light at peak absorption wavelengths.

Several studies on fabricating such devices have been performed to date. The mesoporous metal oxide structure can be fabricated first by solution casting and sintering of nanoparticles, followed by intercalation of the conjugated polymer into the porous structure by spin coating or soaking in solution. The thermodynamics of polymer intercalation into porous media is governed by several driving forces. Osmotic pressure drives polymer chains into the pores. However, the entropic force is opposite due to the reduced number of configurational states available to the confined polymer. The force that can tip the scales in either direction is an enthalpic drive arising from a strong attractive interaction between the polymer and the pore surface, such as one associated with a polar surface and a polarizable polymer.

A strong motivating factor for research on conjugated polymer/metal oxide composite devices is the tremendous amount of recent progress on low-cost, solution-based synthetic routes to novel metal oxide nanostructures.<sup>12</sup> Fabrication of nanotubes and nanorods has been demonstrated for a wide range of oxides, including  $\text{TiO}_2$ ,  $\text{ZnO}$ ,  $\text{SnO}_2$ , and  $\text{GaO}$ , by means of hydrolysis or thermal decomposition pathways of precursors in solution (Figure 3). These can often be nucleated on the surface of the substrate and grown vertically, opening up the possibility of fabricating nanostructures that are optimized for transporting charges to the electrodes.

## Conclusion

Nanostructured *p-n* junctions are a relatively new approach to designing low-cost photovoltaic devices. A wide class of solution-processable semiconductors, both inorganic and organic, have become available. The main attraction of this technology originates in its huge potential for solution processing. First results with respect to photovoltaic devices are encouraging, and better control over morphology on the

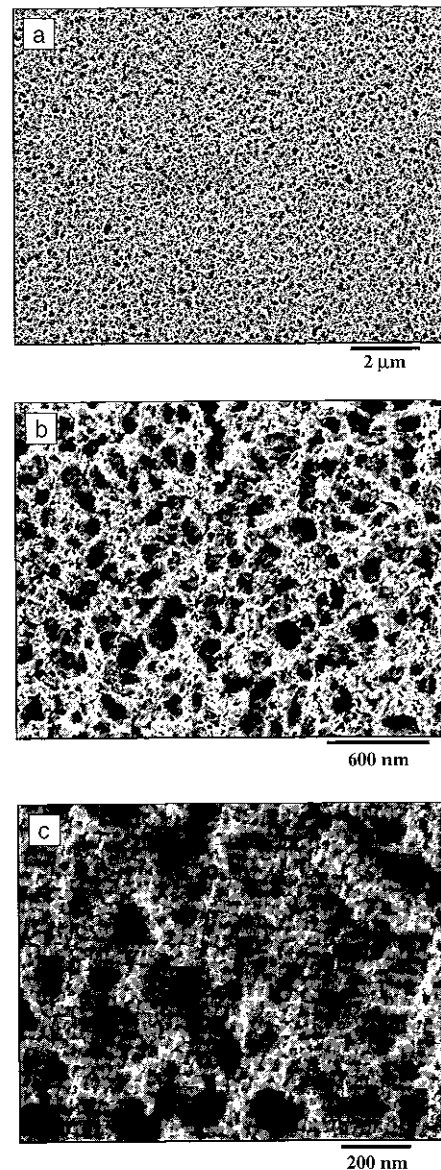


Figure 3. (a)–(c) Scanning electron microscopy images of a nanoporous  $\text{SnO}_2$  network at different resolutions. The structure was fabricated by spin-coating an aqueous solution of  $\text{SnO}_2$  nanoparticles (diameter,  $\sim 9 \text{ nm}$ ) blended with polystyrene spheres (diameter,  $\sim 100 \text{ nm}$ ). Sintering the film at  $450^\circ\text{C}$  in air burned away the polystyrene spheres and caused the  $\text{SnO}_2$  nanoparticles to fuse together to form a continuous network.

nanometer scale is expected to bring further performance improvements.

## References

1. G. Yu, J. Gao, J.C. Hummelen, F. Wudl, and A.J. Heeger, *Science* **270** (1995) p. 1789; M. Granström, K. Petritsch, A.C. Arias, A. Lux,

M.R. Andersson, and R.H. Friend, *Nature* 395 (1998) p. 257.

2. S.E. Shaheen, C.J. Brabec, N.S. Sariciftci, F. Padinger, T. Fromherz, and J.C. Hummelen, *Appl. Phys. Lett.* 78 (2001) p. 841.

3. P. Schilinsky, C. Waldauf, and C.J. Brabec, *Appl. Phys. Lett.* 81 (2002) p. 1.

4. C.J. Brabec, S.E. Shaheen, C. Winder, N. Sariciftci, and P. Denk, *Appl. Phys. Lett.* 80 (2002) p. 1.

5. C.B. Murray, D.J. Norris, and M.G. Bawendi, *J. Am. Chem. Soc.* 115 (1993) p. 8706.

6. W.U. Huynh, J.J. Dittmer, and A.P. Alivisatos, *Science* 295 (2002) p. 2425.

7. B. O'Regan and M. Grätzel, *Nature* 353 (1991) p. 737.

8. K. Murakoshi, R. Kogure, Y. Wada, and S. Yanagida, *Sol. Energy Mater. Sol. Cells* 55 (1998) p. 113.

9. A.F. Nogueira, J.R. Durrant, and M.A. De Paoli, *Adv. Mater.* 13 (2001) p. 826.

10. B. O'Regan, F. Lenzmann, R. Muis, and J. Wienke, *Chem. Mater.* 14 (2002) p. 5023.

11. J. Krüger, R. Plass, M. Grätzel, and H.-J. Matthieu, *Appl. Phys. Lett.* 81 (2002) p. 367.

12. S.E. Shaheen and D.S. Ginley, "Photovoltaics for the Next Generation," in *Encyclopedia of Nanoscience and Nanotechnology*, edited by J.A. Schwarz, C.I. Contescu, and K. Putyera (Marcel Dekker, New York, 2004) in press.

13. M.T. Rispens, A. Meetsma, R. Rittberger, C.J. Brabec, N.S. Sariciftci, and J.C. Hummelen, *Chem. Commun.* (2003) p. 2116. □

The New

## 2004 MRS PUBLICATIONS CATALOG

is in the mail

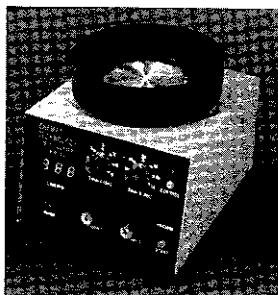
Not an MRS member?

Contact MRS and request a copy today!

[info@mrs.org](mailto:info@mrs.org) or 724-779-3003



## Cost-Effective Portable Spin Coater



### Two-Stage Spinning

Dispense liquid during Stage 1  
Spin-up and flatten during Stage 2

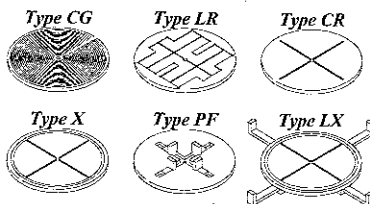
### Adjustable Speed

#### Stage 1

500 to 2500 rpm  
2 to 18 seconds

#### Stage 2

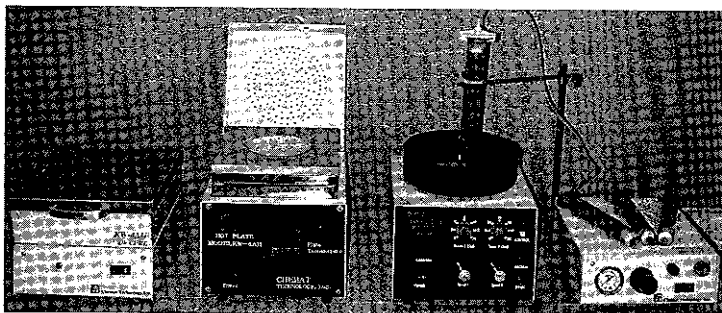
1,000 to 8,000 rpm  
3 to 60 seconds



### Vacuum Chucks

Wide Range of Vacuum Chucks  
Available To Hold Different  
Substrates in KW-4A Spin  
Coater

### KW-4A SERIES PRODUCT LINE



UV Curer  
KW-4AC

Hot Plate  
KW-4AH

Spin Coater  
KW-4A

Dispenser  
KW-4AD



**CHEMAT TECHNOLOGY, INC.**

9036 Winnetka Avenue, Northridge, CA 91324

1-800-475-3628, Fax: 818-727-9477

website: [www.enlabproducts.com](http://www.enlabproducts.com) ; [www.chemat.com](http://www.chemat.com)

email: [marketing@chemat.com](mailto:marketing@chemat.com)

# JMR

because  
important  
work  
deserves  
to be  
published  
quickly

See page 66  
for more information